

Targeting of the Retinal Pigment Epithelium (RPE) by Means of a Rapidly Scanned Continuous Wave (CW) Laser Beam

Ralf Brinkmann,^{1*} Norbert Koop,¹ Mustafa Özdemir,¹ Clemens Alt,¹ Georg Schüle,¹ Charles P. Lin,² and Reginald Birngruber¹

¹Medical Laser Center Lübeck, 23562 Lübeck, Germany

²Wellman Laboratories of Photomedicine, Massachusetts General Hospital, Harvard Medical School, Boston, Massachusetts 02114

Background and Objectives: Selective treatment of the retinal pigment epithelium (RPE) by repetitively applying green μ s-laser pulses is a new method for retinal diseases associated with a degradation of the RPE, which spares the neural retina. We investigated an alternative approach to realize repetitive μ s-laser exposure by rapidly scanning a continuous wave (CW)-laser beam across the RPE.

Study Design/Materials and Methods: An Ar⁺ laser beam (514 nm) with a diameter of 18.75 μ m was repetitively scanned across porcine RPE samples in vitro providing an irradiation time of 1.6 μ s per point on the central scan axis. RPE cell damage was investigated by means of the fluorescence viability assay Calcein-AM.

Results: The ED₅₀ cell damage is 305 mJ/cm² when applying 10 scans with a repetition rate of 500 Hz. The threshold decreases with the number of scans, a saturation was found at 135 mJ/cm² with more than 500 exposures applied. The depth of focus in beam direction is 350 μ m, defined by an increase of the threshold radiant exposure by 20%.

Conclusions: Targeting of pigmented cells with high local resolution has been proved with a laser-scanning device. Looking ahead selective RPE-treatment, the adaptation of a laser-scanning device on a slit-lamp or into a modified retina angiograph seems to be an attractive alternative to the pulsed μ s laser device. *Lasers Surg. Med.* 32:252–264, 2003. © 2003 Wiley-Liss, Inc.

Key words: fluorescence microscopy; melanosome; laser scanner; RPE damage; selective treatment; photocoagulation; viability assay

INTRODUCTION

The concept of selective targeting of naturally or artificially pigmented cells or organelles in less strong absorbing surroundings was introduced by Anderson and Parrish [1,2] and led to a variety of applications in ophthalmology [3,4] and dermatology [2] using pulsed laser radiation. Selective cell effects are most interesting in cases where highly sensitive cells, which have to be preserved, are close to the target cells. As an example of such an application, in vitro targeting of the retinal pigment epithelium (RPE) in the fundus of the eye has been investigated in this study

by means of a scanning application using continuous wave laser radiation.

A variety of retinal diseases such as diabetic macular edema, drusen, and central serous retinopathy are thought to be caused by a decreased function of the RPE. A method for selective destruction of RPE cells without producing adverse effects to adjacent tissue, especially to the neural retina and the choroid, seems to be an appropriate method of treatment [5], presuming that the destroyed cells will be replaced by proliferation or migration of neighboring intact RPE cells.

Selective RPE damage can be obtained due to the fact that the melanosomes inside the RPE cell absorb about 50% of the incident light in the green spectral range [6] and thus are the dominant chromophores within the fundus of the eye. When laser pulses with appropriate energy are applied, high temperatures are induced at the melanosomes. In case of μ s pulse duration, the high temperature is confined to the RPE and leads to the selective RPE cell damage, while only a low sublethal temperature increase is obtained in the adjacent tissue structures [5]. With respect to the origin of cell damage, we refer to Discussion.

The selective damage of the RPE has first been demonstrated by Roeder in rabbits by using 10–500 Argon-ion laser pulses of 5 μ s duration at a repetition rate of 500 Hz [4]. Fluorescein angiography was accomplished to visualize the ophthalmoscopically invisible effects. Two weeks after treatment, the lesions were covered by a new population of RPE cells. Four weeks post-treatment; a morphologically completely restored RPE barrier showing normal RPE cells was found [4]. The selectivity of damage to RPE cells sparing the photoreceptors was demonstrated by histologic examinations at different times after treatment.

Contract grant sponsor: NIH (CPL); Contract grant number: EY12970.

*Correspondence to: Ralf Brinkmann, Medical Laser Center Lübeck GmbH, Peter-Monnik-Weg 4, D-23562 Luebeck, Germany. E-mail: brinkmann@mll.mu-luebeck.de

R. Birngruber has disclosed a potential financial conflict of interest with this study.

Accepted 19 November 2002

Published online in Wiley InterScience

(www.interscience.wiley.com).

DOI 10.1002/lsm.10150

A first clinical trial using a train of μ s-laser pulses from a frequency doubled Nd:YLF laser (wavelength 527 nm, pulse duration 1.7 μ s, 30 or 100 pulses applied at a repetition rate of 100 or 500 Hz, respectively, on a retinal spot of 160 μ m in diameter) has already proved the concept of selective RPE effects and demonstrated the clinical potential of this technique [7,8]. Angiographically determined threshold radiant exposures are around 500 mJ/cm² per pulse. For the treatment typically 650 mJ/cm² are used, however, in order to compensate for the variation in pigmentation and ocular transmission. Microperimetry showed no loss of retinal light sensitivity in the follow-up period and demonstrated the functional selectivity of this technique [9,10].

Since the selective effects in the RPE only rely on local high temperatures within these cells [11], this goal should also be obtained with a continuous wave (CW) laser beam of sufficient irradiance, which is rapidly scanned across the RPE. Combining a commonly available CW green laser, as it is used for routine retinal photocoagulation, with a sharp focusing and fast scanning device, such a system might be suited to also induce selective RPE effects. An advantage of scanning laser over μ s-pulsed application is the possibility to induce RPE defects in an arbitrary pattern within the irradiated areas, thus investigating the therapeutically most useful irradiation geometry.

The aim of this study was to investigate whether scanned CW-laser irradiation can be used to induce RPE effects and

whether RPE-cell damage thresholds are similar to a large area but pulsed irradiation, which are known from previous work [11]. In that study, the damage thresholds of porcine RPE in vitro were determined for the following set of irradiation parameters: 527 nm wavelength (frequency doubled Nd:YLF-laser), 500 Hz pulse repetition rate, 50 μ m laser spot diameter with a top-hat beam profile. For pulse durations of 1 and 3 μ s and application of 10–500 pulses, ED50 threshold radiant exposures between 100 and 160 mJ/cm² were found [11] (compare Fig. 4) [11]. In this setup, we used a small but also spatially top-hat beam profile with a scanning speed to provide a μ s illumination time on the RPE cells. Temperature calculations were performed for a scanned spatially top-hat and Gaussian beam profile in order to assess possible clinical laser scanning devices.

MATERIALS AND METHODS

Experimental Setup

In order to evaluate RPE damage thresholds on porcine RPE samples, we used a setup as sketched in Figure 1. An Ar⁺-Laser (Spectra Physics, Inc., Mountain View, CA USA, model 2030-15s) operated at the wavelength of 514 nm with a maximum power of 7 W served as CW-laser source. The beam was coupled to a 25- μ m core diameter fiber (Fibertech GmbH, Berlin, Germany AS25, NA = 0.1). The length of the fiber was 200 m in order to reduce spatial intensity modulations (speckle) at the distal fiber tip. The fiber tip

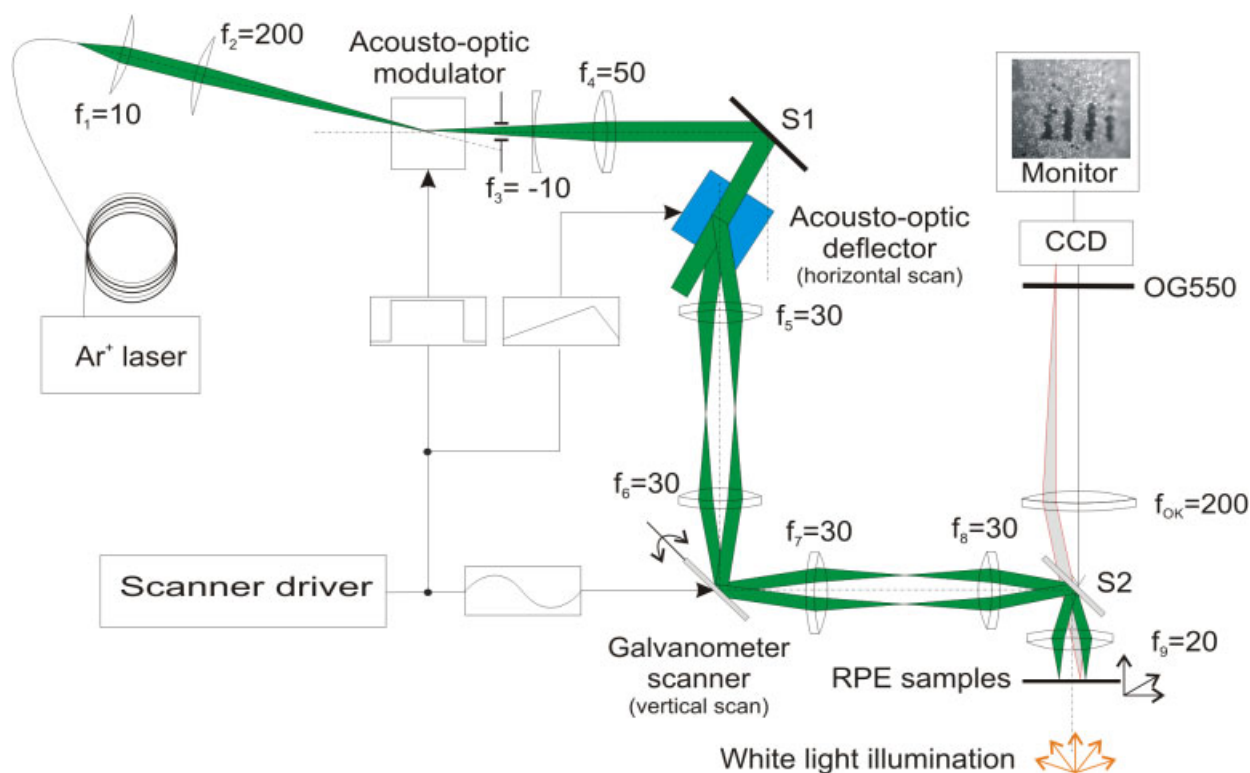


Fig. 1. Experimental setup of the laser scanning system including sample illumination. The focal lengths f of the different lenses is given in millimeters. [Color figure can be viewed in the online issue, which is available at www.interscience.wiley.com]

was imaged onto the object plane with a magnification of 0.75 according to the optical setup shown in Figure 1, yielding a theoretical spot diameter of $2\omega_0 = 18.75 \mu\text{m}$. In order to minimize aberrations, a double telecentric 4-f-optic was used in the scanned beam path. The scanning field for this arrangement was $280 \mu\text{m} \times 280 \mu\text{m}$. The total power P of the beam was measured with a power meter (Coherent, Inc., Santa Clara, CA USA).

An acousto-optic deflector (AOD) (Crystal Technologies, Palo Alto, CA USA AODF 4100-1, 50 MHz bandwidth) provides the fast line scan of 11.7 m/s on the sample to achieve an illumination time of 1.6 μs per point in the central line of the scan. The scanning speed was determined by scanning the beam in the image plane across an object scale and measuring the time between the fringes with a photodiode mounted below. The complete line scan takes 40 μs , while for only 24 μs the beam was on. The vertical scan was provided by a galvanometer scanner (General Scanning, Watertown, MA USA G120D) operated at a frequency of 500 Hz, which subsequently was the framing rate of the repetitive illumination. Since a complete field scan only requires 640 μs , the nearly linear regime of the sinusoidal angle deflection curve can be used. The acousto-optic modulator (AOM) (Landwehr Electronic GmbH, Norderstedt, Germany, M85, 85 MHz) served to block the irradiation in unwanted areas such as the return path of the beam and between irradiated lines. The synchronization of the scanners and the number of illuminated lines was provided by a control unit. The reproducibility to exactly irradiate the same lines with the following scans is within a lateral deviation of maximal 1 μm and in axial direction of $<0.5 \mu\text{m}$.

Determination of the Radiant Exposure on the RPE

When scanning a circular beam of power P with a radius ω_0 and a velocity v in direction z across the target, the radiant exposure $H(x)$ at each point in the scan field decreases with distance x from the central scan axis according to:

$$\begin{aligned} H(x) &= \frac{2P}{\pi \cdot \omega_0^2 \cdot v} \cdot \sqrt{(\omega_0^2 - x^2)} \text{(top hat)} \quad H(x) \\ &= \sqrt{\frac{2}{\pi}} \cdot \frac{P}{\omega_0 \cdot v} \cdot e^{-\frac{x^2}{\omega_0^2}} \text{(Gaussian)} \end{aligned} \quad (1)$$

ω_0 represents the spot radius for a spatially top-hat profile or the Gaussian beam radius, when applying a TEM₀₀ laser beam. The irradiation time on the scan axis is $\tau = 2\omega_0/v$. Thus, for example, to deliver a radiant exposure of $H(0) = 100 \text{ mJ/cm}^2$ at the scan axis ($x=0$) with an illumination time of $\tau = 1.6 \mu\text{s}$ and a scanning spot diameter $2\omega_0 = 18.75 \mu\text{m}$, a laser power of $P = 173 \text{ mW}$ for the top hat and $P = 138 \text{ mW}$ for the Gaussian beam profile is required. If a decrease of the maximum radiant exposure $H(0)$ by 20% perpendicular to the scan axis is tolerated, a stripe with a broadness of 33% of the beam diameter is covered in the Gaussian application mode, while it is 61% in the top-hat case.

If laser light is transmitted by multimode optical waveguides, the intensity at the distal fiber tip is spatially modulated, owing to coherent interference of different fiber modes propagating on different fiber path lengths. Here, the intensity distribution at the fiber tip is imaged onto the object plane. Due to beam deflection and aberrations along the long light path in the scanner, a non-ideal image of the fiber tip is obtained at the probe. The spot diameter and its intensity distribution at the object plane were measured with a CCD-camera using a $40 \times$ magnification, without operating the scanner. The beam profile was analyzed with a beam analyzing software (Polytec GmbH, Waldbronn, Germany, LBA-100).

Figure 2a shows a typical intensity profile, which is scanned across the RPE. Due to spatial aberrations and the intensity modulation, equation 1 cannot be used to properly calculate the radiant exposure $H(x)$ each point in the scanned field experiences. An accurate way to determine the radiant exposure for a scanned beam of arbitrary shape and modulation is described below and used in this study: If a beam with an intensity profile $I(x,z)$ is scanned with the speed v in z -direction over the probe, any point in the scan field experiences the radiant exposure $H_{\text{scan}}(x)$ according to:

$$H_{\text{scan}}(x) = \frac{1}{v} \int I(x,z) \cdot dz \quad (2)$$

Using the intensity distribution $I(x,z)$ achieved from the CCD-image (standing beam), $H_{\text{scan}}(x)$ can be achieved by numerically summarizing the intensity in z -direction:

$$H_{\text{scan}}(x) = \frac{1}{v} \sum_z I(x,z) \cdot \Delta z \quad (3)$$

by normalizing the sum of all camera pixel values $\Phi(x,z)$ to the total incident power P using

$$I(x,z) = \frac{P}{\sum_{\text{pixel}} \Phi(x,z)} \cdot \frac{\Phi(x,z)}{\Delta x \cdot \Delta z} \quad (4)$$

Δx times Δz denote the sizes of a camera pixel, regarding the optical magnification. Figure 2b shows the calculated radiant exposure achieved by summarizing the pixel intensities, shown in Figure 2a, according to equations 3 and 4. The maximal radiant exposure H_{max} , which is not necessarily on the central scan axis, is defined by

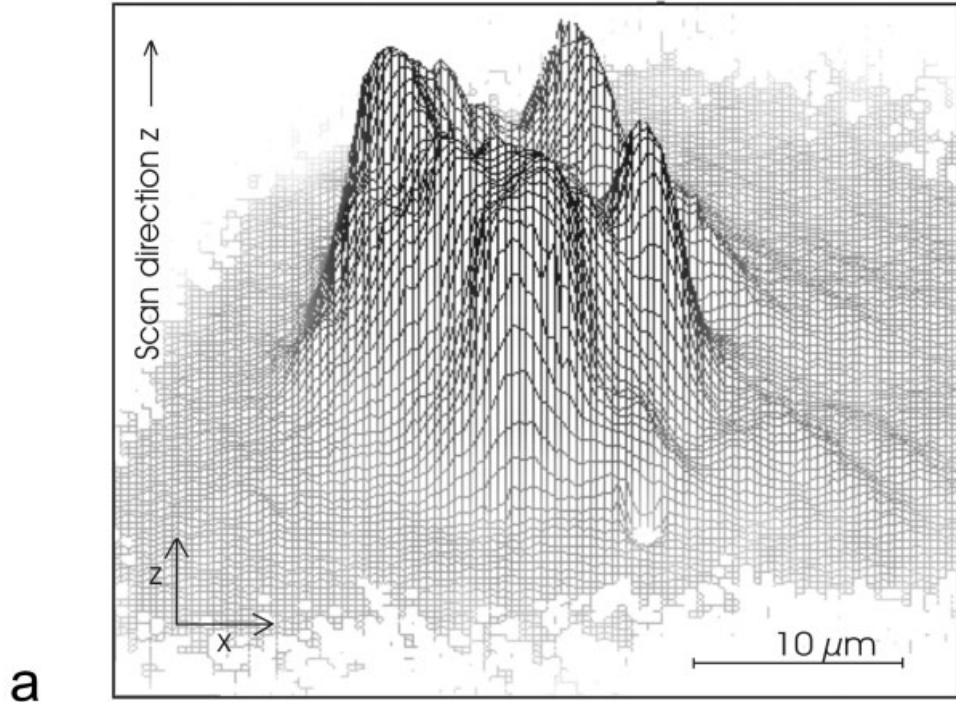
$$H_{\text{max}} = \max(H_{\text{scan}}(x)) \quad (5)$$

The ratio f of this experimental determined value H_{max} to the maximal radiant exposure $H(0)$ of the ideal top-hat beam profile according to equation 1 using $2\omega_0 = 18.75 \mu\text{m}$, is:

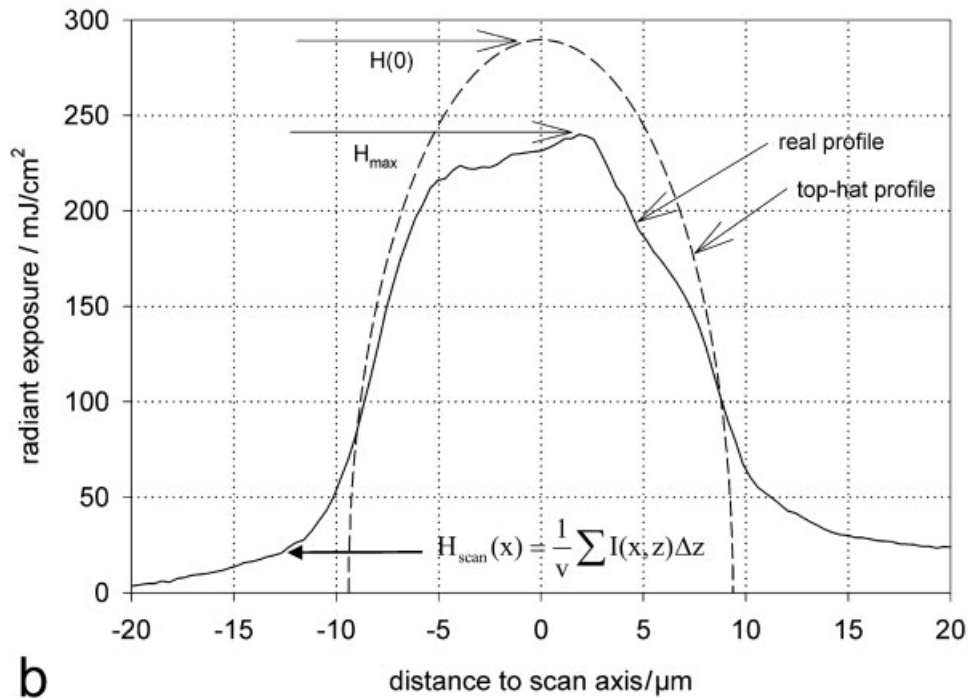
$$f = \frac{H_{\text{max}}}{H(0)} \quad H_{\text{max}} = f \cdot \frac{2 \cdot P}{\pi \cdot \omega_0 \cdot v} \quad (6)$$

Porcine Eye Model and Viability Assay

RPE tissue samples were harvested from freshly enucleated porcine eyes. Stored in cold saline solution, porcine RPE cells survive several hours post mortem. RPE samples were prepared and used for the experiments within 4 hours



a



b

Fig. 2. **a**: The image shows a 3-D intensity plot of the real beam profile at the image plane (specimen). **b**: The solid trace shows the radiant exposure, which each point in the scan field experiences, depending on the distance x of the observation point to the central scan axis. The radiant exposure is obtained by integrating the intensity over time, assuming a scanning

speed $v = 11.7$ m/s of the spot in scan direction (z -direction). Additionally plotted (dashed line) is the radiant exposure, which a non-modulated ideal top-hat beam with a diameter of $18.75 \mu\text{m}$, would provide. It gives a parabolic profile according to equation 1.

post mortem. One circular section of about 1 cm^2 from the fundus of each eye was taken, including retina, sclera, and choroid. The number of sections used to evaluate the threshold data points is indicated in Figure 4. Prior to irradiation, the neural retina was carefully peeled off.

RPE cell viability was probed by the dye Calcein-AM (Molecular Probes, Inc., Eugene, OR USA) that tags living cells. In living cells, Calcein-AM is reduced by esterases to Calcein, which is the actual fluorescent marker. Calcein can be excited with blue light (excitation maximum at 490 nm) to fluoresce in the green spectral region. Calcein-AM was used in a phosphate buffer solution at a concentration of $2 \text{ }\mu\text{g/ml}$. Twenty microliters were dropped onto the RPE cell layer directly after irradiation. Test exposures prior to the study showed the same ED_{50} cell damage thresholds, independent whether Calcein-AM was applied to the sample prior or past irradiation. However, the fluorescence contrast between death and damaged cells was higher when staining after irradiation, since it prevents fluorescence bleaching by the Argon-laser beam. The sample was covered with a microscope cover slip in order to prevent desiccation. The probe was observed 30 minutes after irradiation with a fluorescence microscope. Living cells fluoresce, damaged cells appear dark as exemplary shown in Figure 3b.

Irradiation Modalities and Damage Threshold Determination

The sample was illuminated from the scleral side with white light. The image plane of the scanner and the CCD camera were adjusted to each other. A sharp image of the RPE on the CCD chip was used to adjust the sample to the image plane of the scanner. After sample adjustment, carefully choosing flat areas, four scanning lines were performed on each area as shown in Figure 3b. For most of the RPE probes, several scan fields could be applied onto one sample. To easily determine damage threshold irradiances of the cells, a power gradient along each scanned line, as shown in Figure 3a, was provided by linearly decreasing the diffraction efficiency of the acousto-optic deflector over the length of a scan line.

The cell damage thresholds were determined by measuring the length of the line of damaged cells, d_{th} , with respect to the length of the complete scanned field, $d_{\text{field}} = 280 \text{ }\mu\text{m}$. For evaluation, at least, two damaged cells have to be in contact, while single isolated dead cells, which were often found randomly distributed on the sample, were not considered. The threshold power P_{th} was determined by correlating the line of damaged cells with the power gradient according to Figure 3, using a linear approximation for the power gradient:

$$P_{\text{th}} = P_{\text{high}} - \frac{d_{\text{th}}}{d_{\text{field}}} \cdot (P_{\text{high}} - P_{\text{low}}) \quad (7)$$

The ED_{50} damage radiant exposure H_{th} was determined by inserting P_{th} in equation 6 yielding

$$H_{\text{th}} = \frac{2f}{\pi} \cdot \frac{P_{\text{th}}}{\omega_0 \cdot v} = \frac{f}{\pi} \cdot \frac{P_{\text{th}} \cdot \tau}{\omega_0^2} \quad (8)$$

For each parameter set, samples from 10 different eyes were used. Per eye, several RPE samples could be prepared, which were irradiated at 3–6 different power levels. For the ED_{50} cell damage radiant exposure referred to in Figures 4 and 5, the mean values with standard deviation were calculated. In order to measure the threshold dependence with respect to deviations of the probe from the image plane of the scanner (proper focusing), the RPE was cut in stripes to achieve large areas of most flat RPE.

Temperature Calculations

Temperature distributions at the melanosomes were calculated using an analytical solution of the equation for heat diffusion in a spherical particle [12]. This model was described by Thompson [13] and in detail with respect to μs irradiation in a previous paper [11]. Melanosomes are modeled by spheres with a diameter of $1 \text{ }\mu\text{m}$ having the thermal properties of the surrounding water. It is assumed that inside the sphere heat is produced spatially homogeneously throughout the volume at constant rate during the laser pulse. The total energy, which is absorbed by a melanosome during irradiation, was calculated by assuming an absorption coefficient of $0.8 \text{ }\mu\text{m}^{-1}$ [11]. Corrections for the higher index of refraction of melanin, Mie scattering, and coherent effects due to the small size of the particles were not made. Light absorption in the choroid was neglected. All calculations were performed on a PC using Mathematica 3.0.

RESULTS

A typical plot demonstrating the intensity distribution $I(x,z)$ in the beam profile at the image plane is shown in Figure 2a. Figure 2b shows the radiant exposure, which each point in the scan field experiences, related to its distance x to the central scan axis, using equations 3–5. The parabolic profile is a plot of the ideal top-hat profile according to equation 1. The ratio $f = 0.90 \pm 0.06$, as defined in equation 6, was determined as an average value with standard deviation evaluated out of 20 CCD frames. It is interesting to note that $f < 1$, even though speckle formation takes place, which normally leads to $f > 1$. The reason for the small f is spherical aberration resulting from the non-ideal image of the distal fiber tip, which leads to much a broader beam as the theoretical beam diameter of $2\omega_0 = 18.75 \text{ }\mu\text{m}$ in the image plan, as demonstrated in Figure 2.

Figure 3b shows an example of the scan field in fluorescence microscopy with four illuminated scan lines, the power gradient as shown Figure 3a was applied along the scan direction. The irradiation was performed with 100 scans. The mesh of RPE cells is clearly visible; the dark, non-fluorescing cells were defined as damaged. The length of the damaged line of cells was evaluated to determine the threshold power according to Figure 3a and equation 7.

Figure 4 shows the cell damage ED_{50} radiant exposure for applying 10, 50, 100, 300, 500, 750, and 1,000 repetitive exposures to the RPE. Applying 10 exposures, $P_{\text{th}} = 569 \text{ mW}$ was found, which results in an ED_{50} threshold

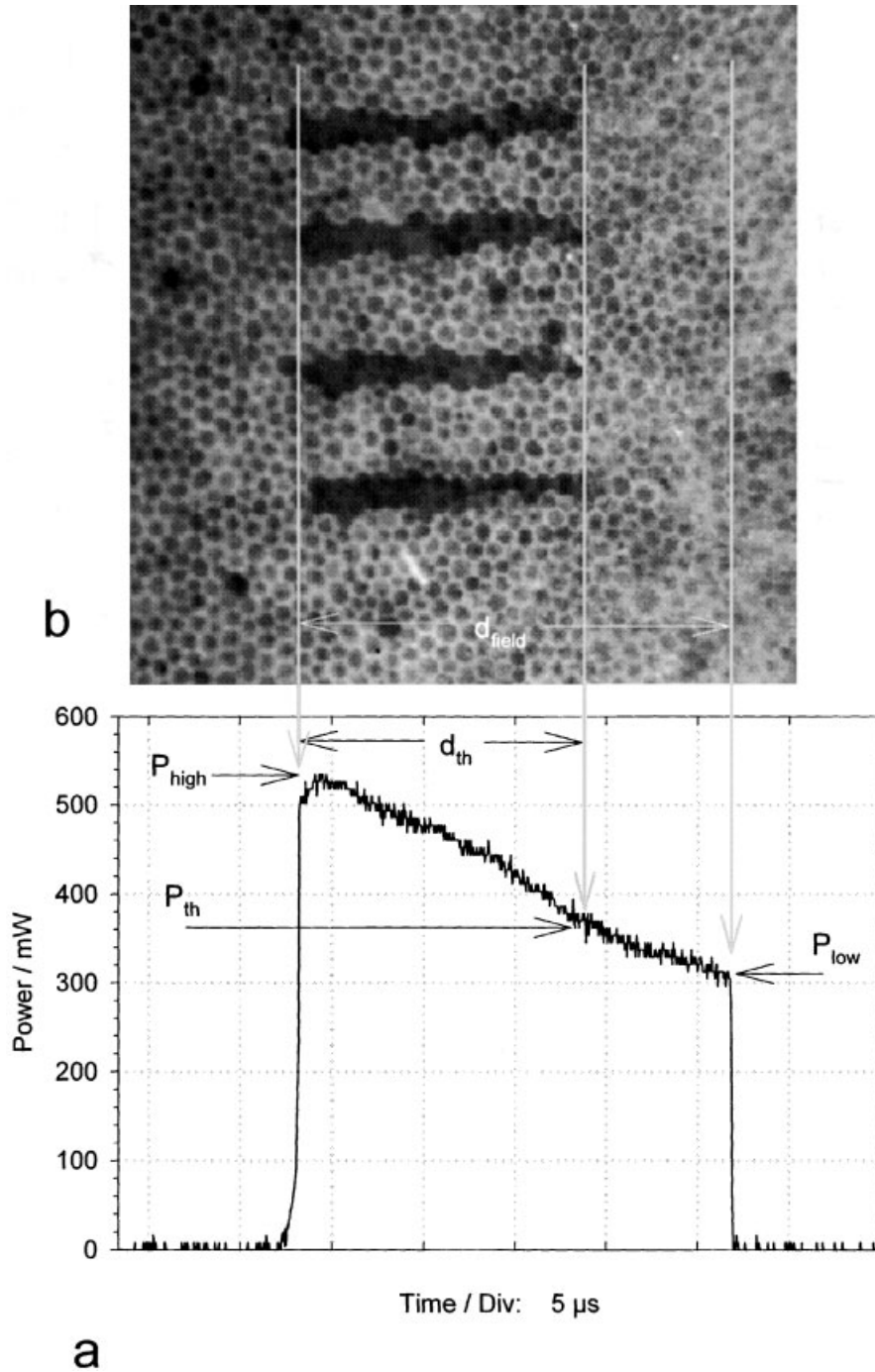


Fig. 3. **a:** A power gradient was applied in scan direction. The complete scan time over the length of a line, $d_{field} = 280 \mu m$, takes 24 microseconds, the peak power (in this case 535 mW) is reduced by 43% over the scan line. For a line of damaged cells

with the length d_{th} , the threshold power P_{th} was determined as sketched. **b:** Typical scan of damaged RPE cells by applying 100 exposures (complete dark hexagons) using fluorescence microscopy. The scan direction was from the left to the right side.

radiant exposure of $H_{th} = 297 \text{ mJ/cm}^2$, as calculated using equation 8. The threshold strongly decreases to $H_{th} = 131 \text{ mJ/cm}^2$ when applying 500 scans, while a higher number of scans does not lead to a further threshold decrease. The solid line in Figure 4 represents a least

square fit of the threshold data according to the empirical function $ED_{50}(N) = ED_{50}(1) * N^{-0.25}$, which is commonly used to determine the additive effect of multiple exposures. N refers to the number of exposures applied, $ED_{50}(1) = 584 \text{ mJ/cm}^2$ is calculated. For comparison, the threshold

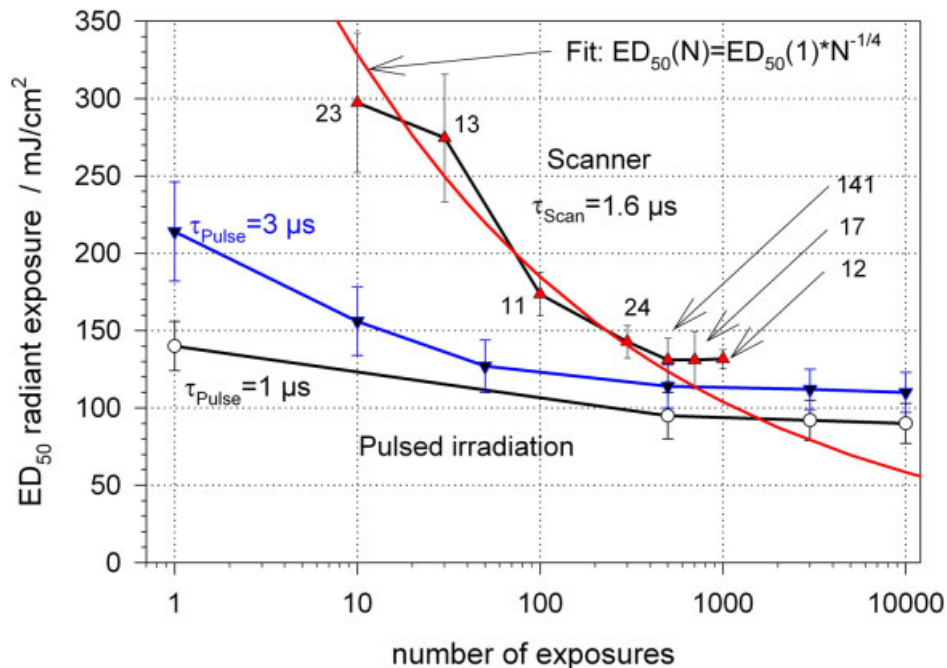


Fig. 4. ED₅₀ RPE threshold radiant exposures as a function of number of exposures for the scanned mode (upper curve) and the pulsed mode with pulse durations of 1 and 3 μs according to [11], respectively. A N^{-1/4}-least square fit was plotted through the scanner data. The numbers indicated in the figure refer to the number of samples (= number of eyes) used to evaluate the data point. [Color figure can be viewed in the online issue, which is available at www.interscience.wiley.com]

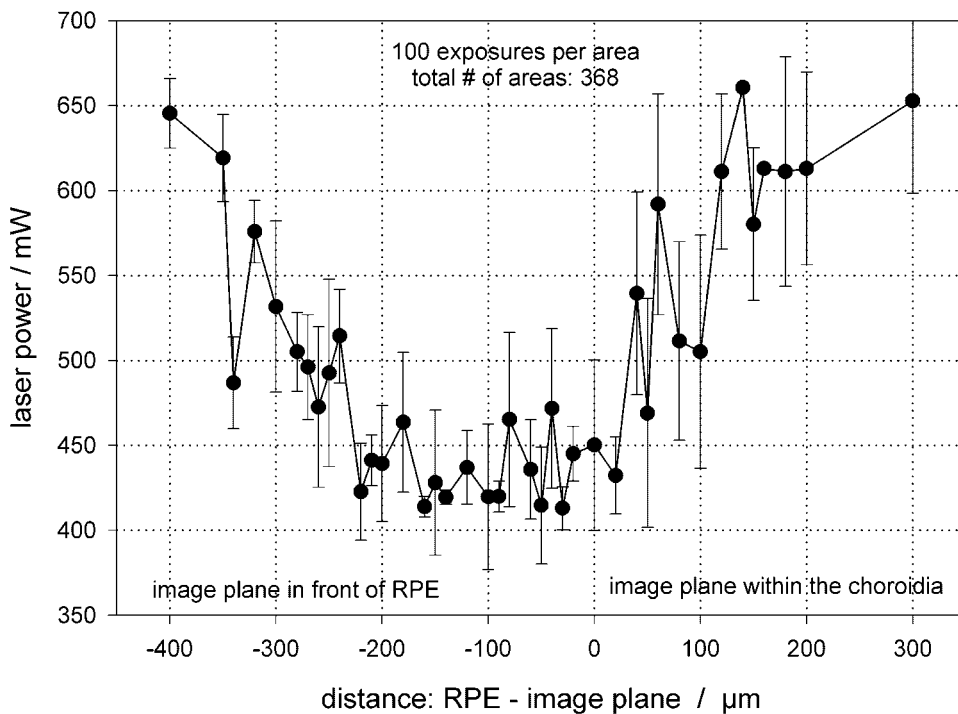


Fig. 5. Laser power at RPE damage threshold depending on the distance of the probe to the image plane.

data achieved with the pulsed setup using 1 and 3 μs pulse durations are also shown [11].

The distance between the sample and the image plane of the scanner was varied in order to determine the damage threshold laser power with respect to proper focusing in the axial direction. This dependence is shown in Figure 5 for 100 exposures per irradiated area. It shows a nearly constant threshold laser power of 420 mW over a range of $\Delta z = 250 \mu\text{m}$, corresponding to $H_{\text{th}} = 218 \text{ mJ/cm}^2$ on the scan axis. Further deviations result in a strongly increasing threshold, 50% in a zone only 100–150 μm outside the central 250 μm zone. In order to enable proper adjustment, very lightly pigmented RPE samples were used in this experiment, which explains the slightly higher threshold radiant exposure compared to $H_{\text{th}} = 173 \text{ mJ/cm}^2$ achieved with stronger pigmented RPE (Fig. 4).

Figure 6 is a plot of the temperature increase at the rim of a melanosome on the scan axis for a beam diameter of 18 μm and a scanning speed of 11.25 m/second. The temperature increases towards its maximum at the end of the irradiation in case of a spatial top-hat beam profile. For a Gaussian profile of the same radius ($1/e^2$) and laser power, a 35% higher temperature is calculated, the maximal temperature is achieved about 400 nanoseconds after the beam center has passed the observation point. With respect to the absolute temperature, it shows that a power of 500 mW under top-hat irradiation conditions is sufficient to induce a temperature increase $\Delta T > 100^\circ\text{C}$ at the melanosomes.

DISCUSSION

The ED_{50} threshold radiant exposure for RPE cell damage by use of a laser scanner has been investigated. A circular spot was repetitively scanned across a porcine RPE layer in vitro with an equivalent exposure time of 1.6 μs per point on the fast scan axis with a framing rate of 500 Hz. The threshold irradiances strongly decrease with increasing number of exposures. However, it is most remarkable that the damage thresholds are significantly higher than in the pulsed application mode under similar irradiation conditions [11]. These results, in comparison to those achieved in the pulsed mode, are analyzed and discussed in the following paragraphs. Furthermore, we describe and discuss possible clinical scanner based treatment systems and judge their features with respect to the pulsed μs laser application system.

Origin of Cell Damage

When laser pulses with appropriate energy are applied to RPE cells, high temperatures are induced in and around the melanosomes. If the vaporization temperature of the intracellular plasma is reached, which takes place at first at the surface of the melanosomes, microbubbles begin to form here. Due to the simultaneous growth of a high number of microbubbles, the cell volume transiently increases, subsequently disrupting the cell structure. Recent investigations demonstrated this effect with nanosecond pulses: Lin et al. experimentally observed microbubble induced

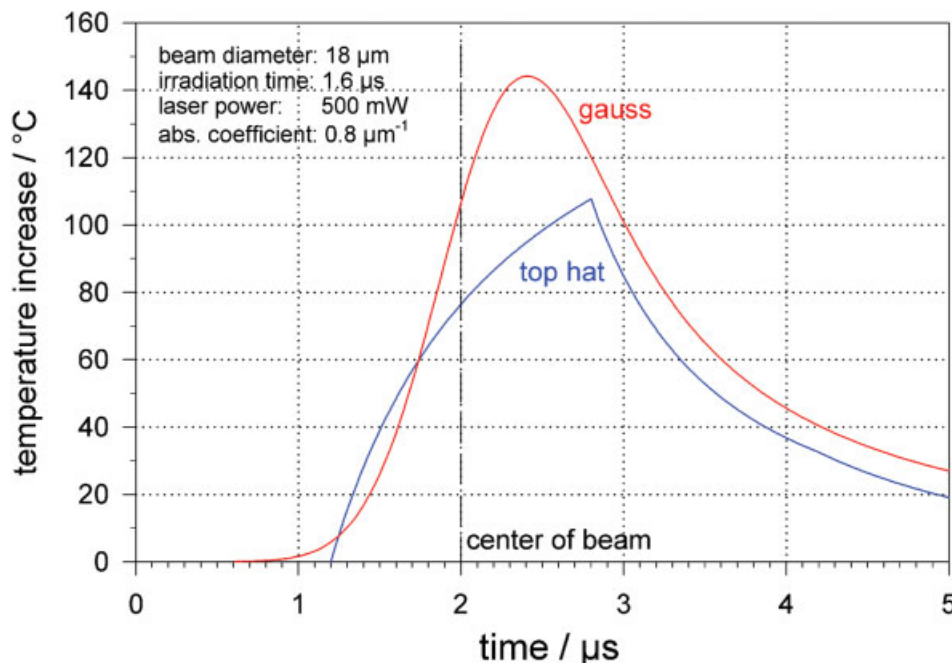


Fig. 6. Calculations of the temperature increase at the rim of an isolated melanosome in suspension on the central scan axis ($x=0$) for scanned Gaussian and top-hat beams with a diameter of 18 μm , a laser power of 500 mW, and a scanning speed of 11.25 m/s, respectively. The dashed line marks the

temperature increase when the center of the beam passes the observation point. The temperature increase is directly proportional to laser power applied. [Color figure can be viewed in the online issue, which is available at www.interscience.wiley.com]

selective cell killing in pigmented cells with nanosecond-pulses [14]. Kelly showed bubble formation inside bovine RPE cells and found that the threshold radiant exposures for bubble formation and for cell death are similar for single picosecond-laser pulses [15]. A recent study with varying pulse durations in the nanoseconds– μ s time range supports the thesis of microvaporization induced RPE cell damage [11].

In order to prove, whether the vaporization threshold might be reached in this approach, temperature estimations were performed for the surface of a single melanosome in water suspension. Figure 6 shows the course of the temperature with a peak increase of $\Delta T = 108^\circ\text{C}$, when using a 500 mW beam with a diameter of $2\omega_0 = 18 \mu\text{m}$ and an exposure time of 1.6 μs . With respect to the cell damage evaluated here: $H_{\text{th}} = 297 \text{ mJ/cm}^2$ (10 exposures) corresponds to an equivalent laser power of 472 mW according to equation 1, thus gives a peak temperature of $T = 124^\circ\text{C}$, incl. room temperature of 22°C . $H_{\text{th}} = 130 \text{ mJ/cm}^2$ (>500 exposures) leads to $T = 67^\circ\text{C}$.

However, for more accurate temperature calculations, the tight mesh of melanosomes inside the RPE cell has to be taken into account. It has been shown that the temperature at a melanosome inside a dense mesh strongly adds up during irradiation due to heat flow from adjacent melanosomes, if pulse durations exceeding the thermal relaxation time of a single melanosome, $\tau_R \approx 400 \text{ ns}$, are used [11].

In conclusion, temperatures above the vaporization threshold of water are most likely induced at cell damage threshold at the melanosomes with the laser parameters used here. Therefore, we assume thermo-mechanical cell disruption owing to microbubble formation as the origin of RPE cell damage and use this thesis in the following sections of Discussion. An overview about other possible mechanisms of RPE cell damage in the μs -time domain is given in the literature but seem to be more unlikely [5,11].

Threshold Dependence on the Number of Exposures

The experiments showed that the threshold radiant exposure for cell damage significantly decreases with the number of exposures, possible reasons shall be discussed here.

For a variety of pulse durations, pulse numbers, and wavelengths it has been shown in the literature that the damage threshold scales with $N^{-1/4}$, when N expositions are applied [16]. This empirically found dependence has been verified by a number of studies on retinal laser damage thresholds [17,18]. Applying this law to our experimental data, the solid line shown in Figure 4 represents a quite good accordance to this law between 10 and 500 scans. With respect to the damage threshold for only one scan, which could not be investigated due to too less laser power available, a radiant exposure of 584 mJ/cm^2 can be calculated. This is nearly two times higher than that for 10 scans, which seems to be very unlikely, if we compare it to the pulsed data shown in Figure 4 with about 30%

threshold increase. Further, the radiant exposure saturation as observed for higher number of exposures does also not obey this law. In conclusion, the $N^{-1/4}$ law can only be applied over a very limited range of 10–500 exposures.

The threshold saturation can also not be explained with the Arrhenius formalism for thermal damage, since it also predicts a steady decrease of the thresholds for increasing exposures. It can also be excluded that an increase of the residual RPE temperature prior to the next exposure leads to a reduced threshold with increasing exposures: RPE temperature estimations for a high number of exposures with a spot diameter of $18 \mu\text{m}$ and a laser power of 500 mW do not result in a significant residual temperature increase: $\Delta T < 5^\circ\text{C}$ after 500 pulses was calculated, thus this effect can be neglected.

A more reasonable explanation for the lower threshold radiant exposure with increasing number of exposures might be the statistical behavior of bubble formation at threshold. Lin proved that RPE cell damage can occur, if only one pulse out of a train of 100 pulses, 6 μs in duration, leads to vaporization.

Cell Selectivity

The selectivity of the method with respect to the neural retina and the photoreceptors could not be investigated with this model and setup. However, Figure 3b shows the lateral selectivity of the irradiation: Even above threshold (begin of the scan line), neighboring RPE cells (typically 10–15 μm in diameter), which were not passed by the laser spot, were not damaged. Thus, mechanical or thermal effects owing to microbubbles or heat diffusion, respectively, originating from the irradiated cells are not sufficient to cause damage to neighboring cells. This selectivity sparing adjacent tissue is much likely also in the axial beam direction towards the adjacent photoreceptors. For the pulsed irradiation, microperimetry performed on patients showed no loss of retinal light sensitivity in the follow-up period and demonstrated the functional selectivity of this technique [9,10], even though the radiant exposure was much higher. It has also been proved by histologic examinations at different times after irradiation of rabbits [4]. In conclusion, photoreceptor damage is most unlikely with such a scanning irradiation mode, if the laser power is kept close above RPE damage threshold.

Threshold Radiant Exposures: Pulsed Versus Scanning Mode

It is most remarkable that although the average radiant exposure for all points on the scan axis is the same in the pulsed and the scanning mode, the thresholds for the scanning irradiation are always higher, up to a factor of 2 for 10 and 50 exposures. In order to understand this discrepancy, a closer analysis of the different irradiation modalities with respect to the origin of cell damage is needed:

1. In contrast to the pulsed mode, not all melanosomes within a cell experience the same radiant exposure, due to the circular spot scanned, as shown in Figure 2. A

radiant exposure within a range of 20% of the maximum radiant exposure is achieved only in a scanned stripe of about 60% of the beam diameter, which is less than a typical cell diameter in this case. Further, most of the cells are not hit totally but only partially due to the fact that spot and the cell size are about equal. This is supported by the observation that at threshold, some damaged cells are often totally surrounded by non-damaged cells.

2. Not all cell melanosomes experience the same radiant exposure at the same time. Most likely, microbubble formation at threshold takes place at the end of the irradiation, when the highest temperature is just reached (Fig. 6). Thus, a front of a few small bubbles moves through the cells at the very rear end of the scanned spot. Therefore, although the radiant exposure per melanosome is similar, the volume increase within the cell is much smaller in the scanning mode in comparison to the pulsed mode.
3. Since the beam profile is not an ideal top-hat profile, the highest temperature is achieved before the beam has totally passed the observation point, comparable to the Gaussian profile (Fig. 5). Thus, the effective radiant exposure until the peak temperature is reached is correspondingly smaller as the values calculated for Figure 4, where the total applied energy was taken into account.

All points most likely contribute to a higher threshold radiant exposure in the scanned mode compared to the pulsed mode, thus the higher thresholds observed seems reasonable. The intensity modulation within the spot due to coherent interference might lead to an increase or decrease of the threshold irradiance, depending on the local distribution of the speckle. The different spot diameter in both cases (50 μm pulsed and 18.75 μm scanned) should play no role, since the temperature increase depends on the radiant exposure. An increase of the average RPE temperature due to repetitive exposures up to 500 Hz can be neglected in both cases.

Laser Scanner for Clinical Applications

The question arises how such a scanner system can be realized for a clinical application. In order to discuss scanning treatment modalities, let us first review the clinically available data for treatment with a pulsed laser by use of a pulse duration of 1.7 μs (see Introduction): It shows that 650 mJ/cm^2 are commonly used for treatment, which is about 30% above the angiographic threshold of about 500 mJ/cm^2 . This is about four times higher than the porcine RPE damage threshold achieved with the same laser using a viability stain as depicted in Figure 4, for 100 pulses applied. Apart from the different methods to determine RPE damage, the higher human threshold is most likely originating from two different facts: First of all, due to the lower melanin pigmentation, the human RPE absorbs 50–60% of light in the green spectral range, while porcine RPE absorbs nearly 100%. Secondly, the direct transmittance of light through the whole human eye has to be kept in

mind in comparison to the in vitro experiments on RPE specimen. Although the total transmittance of light in the green spectral range is around 80%, the direct transmittance (within an angle of 1°) is only 40% due to mostly forward scattering of the ocular media [19].

Further referring to Figure 4, it shows that a 1.5 times higher radiant exposure is needed in the scanning mode compared to the pulsed mode in order to obtain RPE damage, when applying 100 exposures, for reasons discussed above. Assuming that this factor achieved with porcine eyes can be transferred to a clinical treatment, than a radiant exposure of about 750 mJ/cm^2 is needed to reach the angiographic ED_{50} threshold in humans by use of a laser scanner with an illumination time of 1.7 μs . About 1,000 mJ/cm^2 should be used for an efficient treatment.

With respect to the selectivity and thus safety of the treatment, the so-called therapeutic window between angiographic and ophthalmoscopic visibility was investigated in rabbits, showing a safe treatment range between 170 and 430 mJ/cm^2 (527 nm, pulse duration: 1.7 μs , 100 pulses at 500 Hz) [20]. Below this fluence, RPE damage is uncertain (angiographic ED_{50} : $H_{\text{th}} = 138 \text{ mJ}/\text{cm}^2$), while above, extended damage becomes obvious (ophthalmoscopic ED_{50} : $H_{\text{th}} = 480 \text{ mJ}/\text{cm}^2$). Transferring this results to the clinical application, than $\sim 2,500 \text{ mJ}/\text{cm}^2$ should not be exceeded in order to avoid retinal damage.

In order to achieve a radiant exposure of 1,000 mJ/cm^2 with a top-hat spot diameter of 18 μm and an illumination time of 1.6 μs along the scan axis, a laser power as high as 1.6 W according to equation 1 is needed on the RPE, without regarding intensity modulation. However, reviewing equation 8, there are several possibilities to reduce this high laser power:

1. The spot diameter can be reduced, since the laser power needed to achieve the desired radiant exposure is inversely proportional to the spot diameter, if the scanning speed is kept constant (eq. 8). It drops even inversely proportional to the square of the beam diameter, if the illumination time per point is kept constant. However, with respect to the limited optical quality of the eye, the minimal achievable beam diameter on the retina is about 10 μm . Further, with reduced spot diameter, the depth of focus is reduced, the consequences on this are discussed in more detail below.
2. A Gaussian instead of a top-hat beam profile can be used. In this case, about 25% less power is required to obtain the same temperature at the melanosomes on the scan axis according to Figure 6. However, a smaller stripe of melanosomes experiences high temperatures (compare eq. 1), which might lead to an increased damage threshold, since less microbubbles are produced.
3. The illumination time can be increased, since it is reciprocally proportional to the laser power. However, in this case, an increase of the damage threshold is expected, as shown in Figure 4, since the temperature increases slower than proportional with time (Fig. 6) due to increasing thermal diffusion during irradiation

[11]. Further, the therapeutical window becomes significantly smaller. The safety range is reduced to a factor of 1.5 with an illumination time of 5 μs [21].

4. The number of exposures can be increased. In this case, it has to be assured that the same scan line can be irradiated several times, if an irradiation modus of separated scan lines is used. Therefore, micromovements of the eye have to be excluded, thus fundus movements relative to the laser beam path have to be kept smaller than about 10 μm per 300 μs .

Slit Lamp Application

From the technical point of view, all conventional retinal photocoagulations as well as the pulsed selective RPE treatment are performed via a slit lamp with a multimode fiber adapted laser. The laser light is coupled to the eye with a contact lens, which is placed on the cornea to compensate for the refractive power of the eye. In order to achieve a homogeneous energy distribution on the retina, the distal fiber tip with its nearly top-hat intensity profile is imaged with the slit-lamp optics onto the fundus. The axial adjustment Δz (z-adjustment) is performed manually by the ophthalmologist by moving the slit lamp until the laser spot of the pilot laser shows a sharp image on the retina. Under optimal conditions with a narcotized rabbit, we measured a reproducibility of focusing of about $\Delta z = \pm 200 \mu\text{m}$, however, in practice, a much larger range is expected. Even if the slit lamp is properly used with an ocular crossed hair to avoid accommodation mismatch between the ophthalmologist's view and the image plane of the scanned spot, slight eye and patient movements can hardly be avoided. A further drawback is patients with beginning cataract. Due to light scattering, proper focusing to the retina will become difficult and moreover, the scanning spot on the RPE is smeared out, thus damage thresholds are expected to rise strongly. Therefore, cataract patients have to be excluded from treatment. The problem of proper depth adjustment with respect to a safe but effective treatment will be addressed in the following paragraph.

For applying a top-hat beam profile, the analysis is quite complicated, since the beam profile changes in the near field around the image. For an 18.75 μm spot diameter as used here, it is as small as 300 μm when allowing a maximal threshold increase of 20% (Fig. 5). In order to simplify the discussion, we focus on a Gaussian beam application, which can easily be calculated. The TEM_{00} focal beam radius ω_0 and the beam radius ω_z at a distance Δz to the focal plane are related by:

$$\Delta z = \frac{\pi \cdot \omega_0^2}{\lambda} \cdot \sqrt{\left(\frac{\omega_z}{\omega_0}\right)^2 - 1} \quad (9)$$

In order to analyze the change of the radiant exposure by defocusing, we assume that a radiant exposure of 750 mJ/cm^2 is required in order to guarantee treatment (25% less than in the top hat case as discussed above) by use of a scanning speed $v = 2\omega_0/\tau$ with $\tau = 1.7 \mu\text{s}$. Combining equations 8 and 9, the useful range of spot diameter with

respect to laser power and accuracy in depth of focus can be calculated.

Figure 7 shows the decrease in radiant exposure when defocusing for different spot radii. The power was normalized to a radiant exposure of 1,300 mJ/cm^2 in the focus, which is in the center of the therapeutic window. It shows that with $\omega_0 = 5 \mu\text{m}$ spot radius, a power of about 1W is sufficient for RPE damage. But in order to stay within the therapeutic window, the focusing range is only $\pm 200 \mu\text{m}$. If this range shall be increased, a larger spot diameter is required. Using $\omega_0 = 7.5 \mu\text{m}$, the range is extended to $\pm 500 \mu\text{m}$, which can realistically be obtained during treatment; however, the power needed in this case is above 2 W. The power further increases with spot diameter. In conclusion, a beam diameter of $2\omega_0 \approx 15 \mu\text{m}$ seems to be ideal. However, with an additional fast automatic z-tracker, a smaller spot diameter and less power can probably be used.

Retina Scanner Application

Another possible application device makes use of the principle of a retina laser scanner (e.g., the HRA from Heidelberg Engineering GmbH, Germany or the SLO from Rodenstock GmbH, Germany) commonly used for retinal diagnostics. In this case, a collinear beam is illuminated on the cornea, which focuses the laser beam to a minimal spot diameter of approximately 10 μm onto the retina. In this case, axial deadjustment is uncritical and the required laser power may be kept below 1 W for an exposure time of 1.6 μs . However, lateral eye movements have still to be considered in order to make use of the threshold decrease with multiple scans: Movements larger than the spot diameter between the scans will lead to a strong increase of the threshold (Fig. 4), since always different RPE is targeted. In the worst case, RPE-damage has to be provided with a single scan. As a matter of principal, only slight modifications (substantially a small laser and an optoacoustic modulator to switch on the laser at the desired treatment locations) are needed to modify the retina scanner, since their intrinsic scanning rates are in the order of the illumination times needed here. However, up to now retina scanning systems have not been used for treatment. The ophthalmologists have therefore to judge whether a treatment in front of a monitor would be acceptable.

On-line Treatment Control System

A further point to be considered bases on the fact that the selective RPE defects are ophthalmoscopically invisible. Thus an automatic detection system reporting a successful irradiation would be highly useful. The dosimetry is currently performed by fluorescein angiography post treatment, which demarks the RPE barrier defect. By use of a combined RPE treatment and diagnostic system, such a detection could be realized either by autofluorescence changes or by use of exogeneous chromophores applied during or directly after treatment. Moreover, other non invasive detection methods such as optical [21] or optoacoustical [22] on-line dosimetry control devices are under

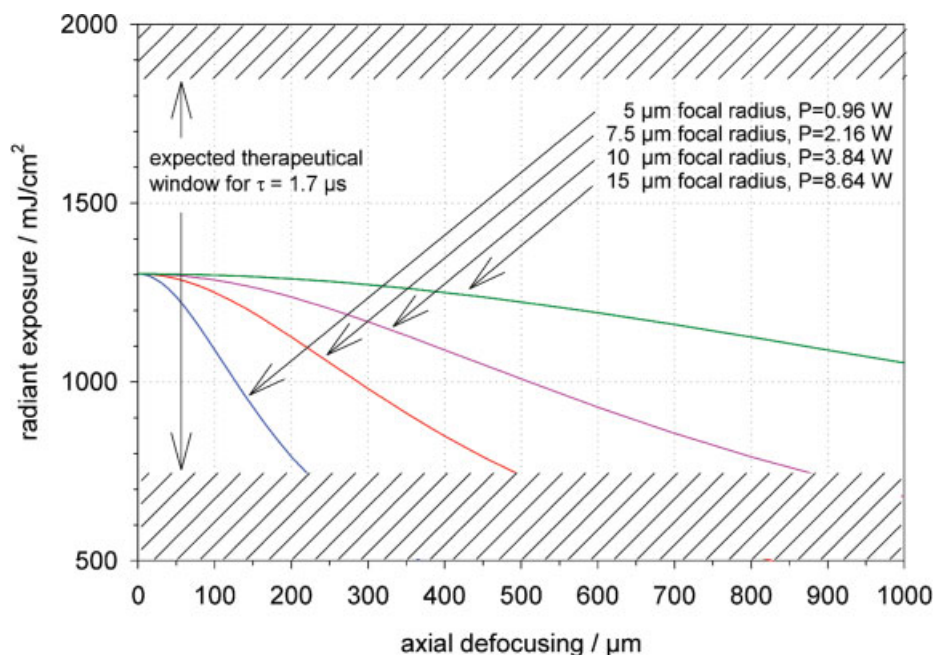


Fig. 7. Radiant exposure on the RPE versus axial defocusing up to 1 mm using a focal illumination time of $1.6 \mu\text{s}$ (defocussing = 0) on the central scan axis for different focal spot radii applied by a slit lamp based scanner using a Gaussian beam. The laser powers indicated on each curve are

normalized to a radiant exposure of $1,300 \text{ mJ/cm}^2$ in the focus, which is around the center of the indicated therapeutical window for an illumination time of 1.6 microseconds. [Color figure can be viewed in the online issue, which is available at www.interscience.wiley.com]

investigation for the pulsed application, but have to be further explored for a scanning device.

CONCLUSION

Damaging of pigmented cells under high local resolution could exemplary be demonstrated on the RPE with a scanning CW laser device. A spot diameter of $18.75 \mu\text{m}$ was scanned with a speed of 11.7 m/s across the RPE using laser powers around 500 mW . The ED_{50} thresholds for porcine RPE damage strongly decrease with the number of exposures applied. From 10 to 500 illuminations, the empirical $N^{-0.25}$ law is an appropriate approximation, however, large deviations are found for higher numbers of exposures. The thresholds are up to a factor of 2 above the corresponding thresholds found for repetitively pulsed irradiation with the same illumination time.

In order to realize a clinical system for selective RPE-treatment, a modified diagnostic laser scanning device would be the first choice, since depth focusing is not required and thus a CW-laser power below 1 W can be expected for an illumination time of about $1.7 \mu\text{s}$. The power can further be reduced by using a slower scanning speed, however, the therapeutic window with respect to RPE cell selective damage will become smaller. A slit lamp adapted scanning unit is also feasible but probably requires an automatic focusing control, if high laser powers shall be avoided. For both devices, lateral eye movements during irradiation have to be kept smaller than the spot diameter, if separated RPE cells or lines of cells shall be targeted.

Otherwise, a strong increase of the RPE damage radiant exposure can be expected. The main advantages of a scanning laser system compared to a pulsed treatment device is its high flexibility to induce arbitrary RPE treatment pattern with a high local resolution. This application system would be optimally suited for investigating the most useful irradiation pattern for treatment of the different RPE related diseases.

REFERENCES

1. Anderson RR, Parrish JA. Selective photothermolysis: Precise microsurgery by selective absorption of pulsed laser radiation. *Science* 1983;220:524–527.
2. Parrish JA, Anderson RR, Harist T, Paul B, Murphy GF. Selective thermal effects with pulsed irradiation from lasers: From organ to organelle. *J Invest Dermatol* 1983;80(6):75–80.
3. Latina MA, Park C. Selective targeting of trabecular meshwork cells: In vitro studies of pulsed and CW laser interaction. *Exp Eye Res* 1995;60:359–372.
4. Roeder J, Michaud NA, Flotte TJ, Birngruber R. Response of the retinal pigment epithelium to selective photocoagulation. *Arch Ophthalmol* 1992;110:1786–1792.
5. Roeder J, Hillenkamp F, Flotte TJ, Birngruber R. Microphotocoagulation: Selective effects of repetitive short laser pulses. *Proc Natl Acad Sci USA* 1993;90:8463–8647.
6. Gabel VP, Birngruber R, Hillenkamp F. Visible and near infrared light absorption in pigment epithelium and choroid. *Congress Series: XXIII Concilium Ophthalmologicum* 1978;450:658–662.
7. Roeder J, Wirbelauer C, Brinkmann R, Laqua H, Birngruber R. Control and detection of subthreshold effects in the first clinical trial of macular diseases. *Invest Ophthalmol Vis Sci* 1998;39(4):104.

8. Roider J, Brinkmann R, Wirbelauer C, Laqua H, Birngruber R. Subthreshold (retinal pigment epithelium) photocoagulation in macular diseases: A pilot study. *Br J Ophthalmol* 2000;84:40–47.
9. Roider J, Wirbelauer C, Brinkmann R, Laqua H, Birngruber R. Variability of RPE reaction in two cases after selective RPE laser effects in prophylactic treatment of drusen. *Graefe's Arch Clin Exp Ophthalmol* 1999;237:45–50.
10. Roider J, Brinkmann R, Wirbelauer C, Laqua H, Birngruber R. Retinal sparing by selective retinal pigment epithelial photocoagulation. *Arch Ophthalmol* 1999;117:1028–1034.
11. Brinkmann R, Hüttmann G, Rögner J, Roider J, Birngruber R, Lin CP. Origin of retinal pigment epithelium cell damage by pulsed laser irradiance in the nanosecond to microsecond time regimen. *Lasers Surg Med* 2000;27(5):451–464.
12. Carslaw HS, Jaeger JC. *Conduction of heat in solids*, second edition. Oxford: Clarendon Press; 1959.
13. Thompson CR, Gerstman BS, Jacques SL, Rogers ME. Melanin granule model for laser-induced thermal damage in the retina. *Bull Math Biol* 1996;58(3):513–553.
14. Lin CP, Kelly MW, Sibayan SAB, Latina MA, Anderson RR. Selective cell killing by microparticle absorption of pulsed laser radiation. *IEEE J select Topics Quantum Electron* 1999;5(4):963–968.
15. Kelly WM, Lin CP. Microcavitation and cell injury in RPE cells following short-pulsed laser irradiation. *Proc SPIE* 1997;2975:174–179.
16. ANSI. 1993. Standard Z136.1: American Standard for the Safe Use of Lasers: American Standards Institute.
17. Ham WT, Mueller HA, Wolbarsht ML, Sliney DH. Evaluation of retinal exposures from repetitively pulsed and scanning lasers. *Health Physics* 1988;54(3):337–344.
18. Stuck BE, Lund DJ, Beatrice ES. 1978. Repetitive pulse laser data and permissible exposure limits. Vol. Report No. 58. San Francisco: Lettermann Army Institute of Research, Presidio of San Francisco.
19. Boettner EA, Wolter JR. Transmission of the ocular media. *Invest Ophthalmol Vis Sci* 1962;1:776–783.
20. Framme C, Schüle G, Roider J, Kracht D, Birngruber R, Brinkmann R. Threshold determinations for selective RPE damage with repetitive microsecond laser systems in rabbits. *Ophthalmic Surg Lasers* 2002;33(5):400–409.
21. Neumann J, Brinkmann R. Interferometric detection of laser-induced microbubbles in the retinal pigment epithelium. In: *Laser-tissue interactions, therapeutic applications, and photodynamic therapy*. van den Bergh, Hubert: Birngruber, Reginald; 2001;. *Proc SPIE* 4433:81–86.
22. Schüle G, Hüttmann G, Roider J, Wirbelauer C, Birngruber R, Brinkmann R. Optoacoustic measurements during μ s-irradiation of the retinal pigment epithelium. *Proc SPIE* 2000;3914:230–236.